

https://dspace.org/

# Phosphide capacities of ferromanganese smelting slags

**Maramba, Blessing**

**2008-04-21T05:28:34Z**
http://hdl.handle.net/10539/4767

Downloaded from a DSpace repository. https://dspace.org/

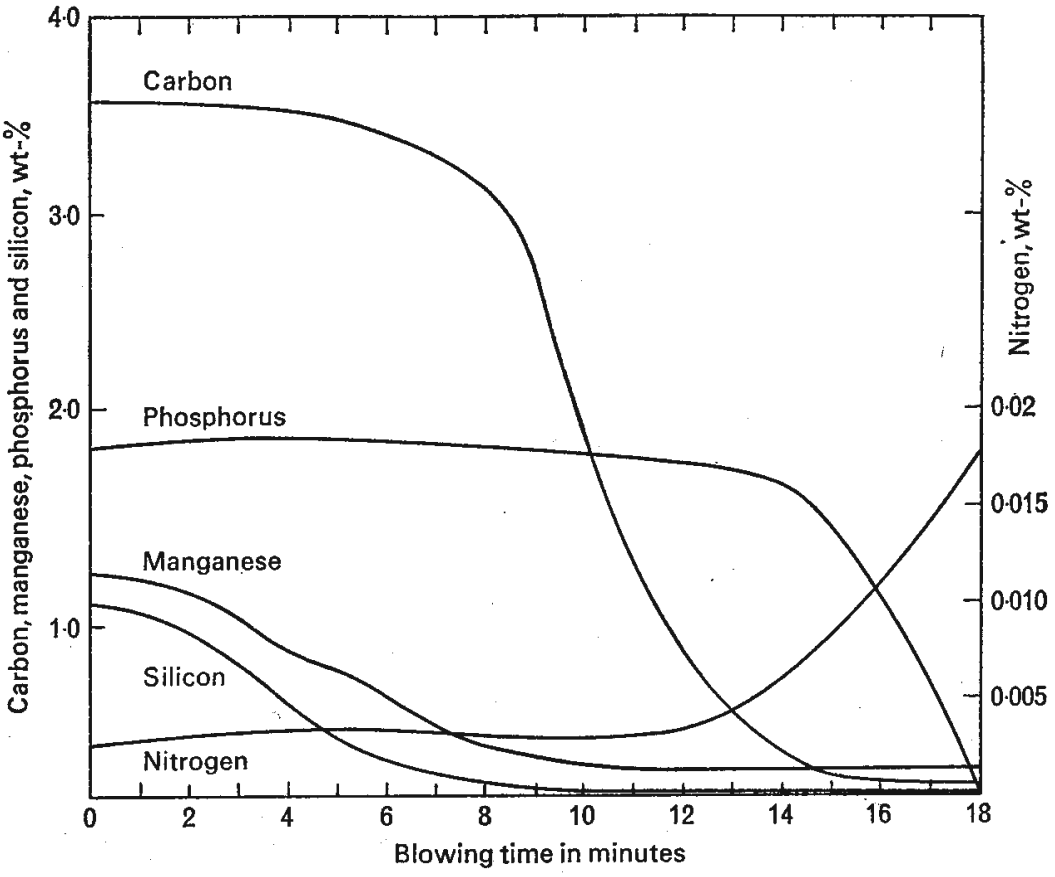



**Figure 2.1** Change of metal composition with time in the "Basic Bessemer process"[7]

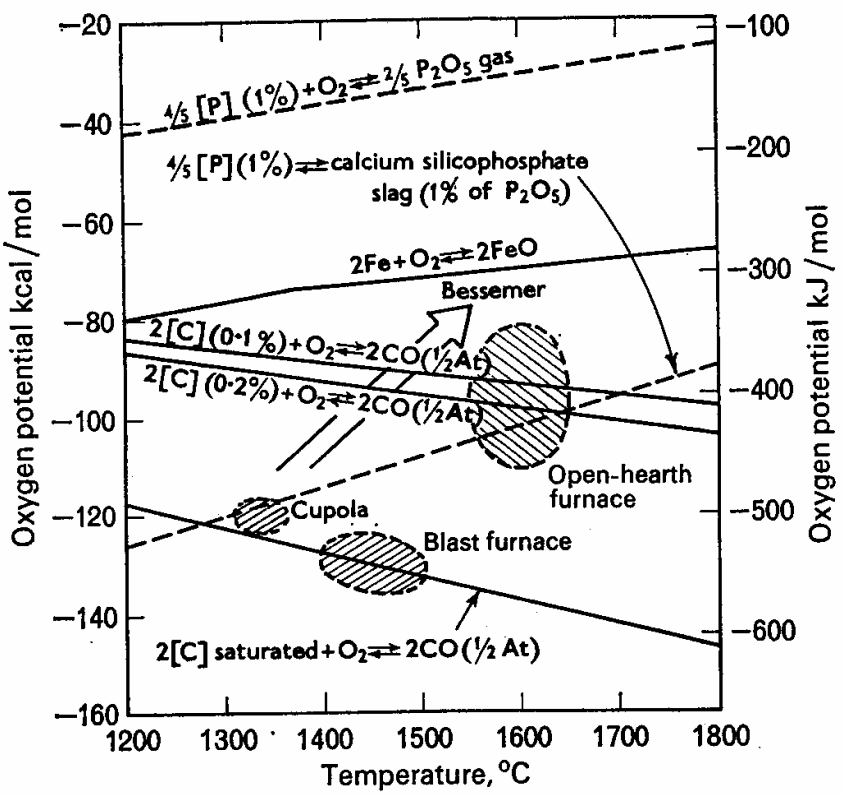



**Figure 2.2** Comparison of the oxygen potentials at which phosphorus can transfer from the metal to slag with the oxygen potentials of various iron and steel making processes[7]

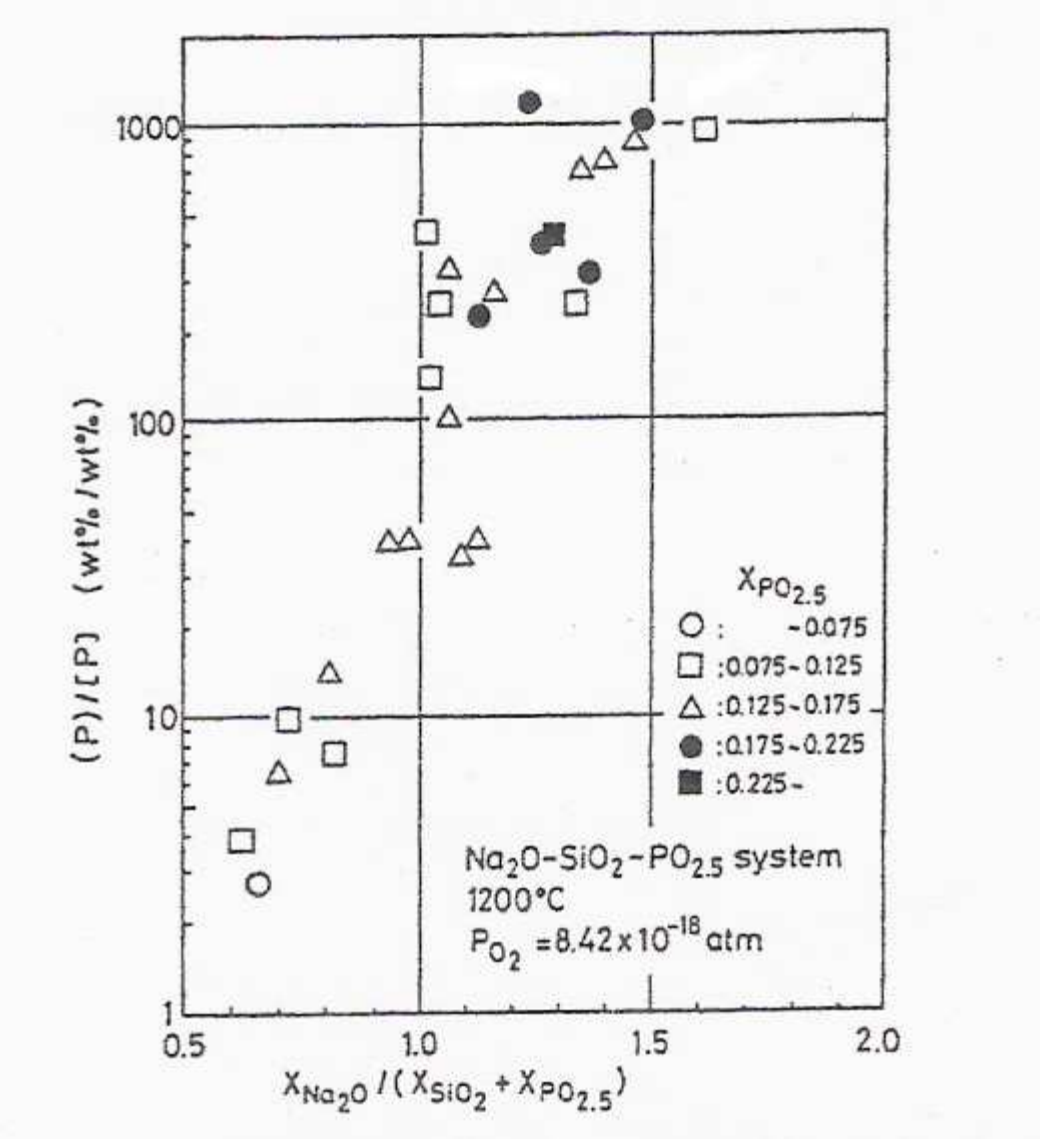



**Figure 2.3** The relationship between phosphorus distribution ratio and $X_{Na_2O}/\left(X_{SiO_2}+X_{PO_{2.5}}\right)$ at 1200°C[11]

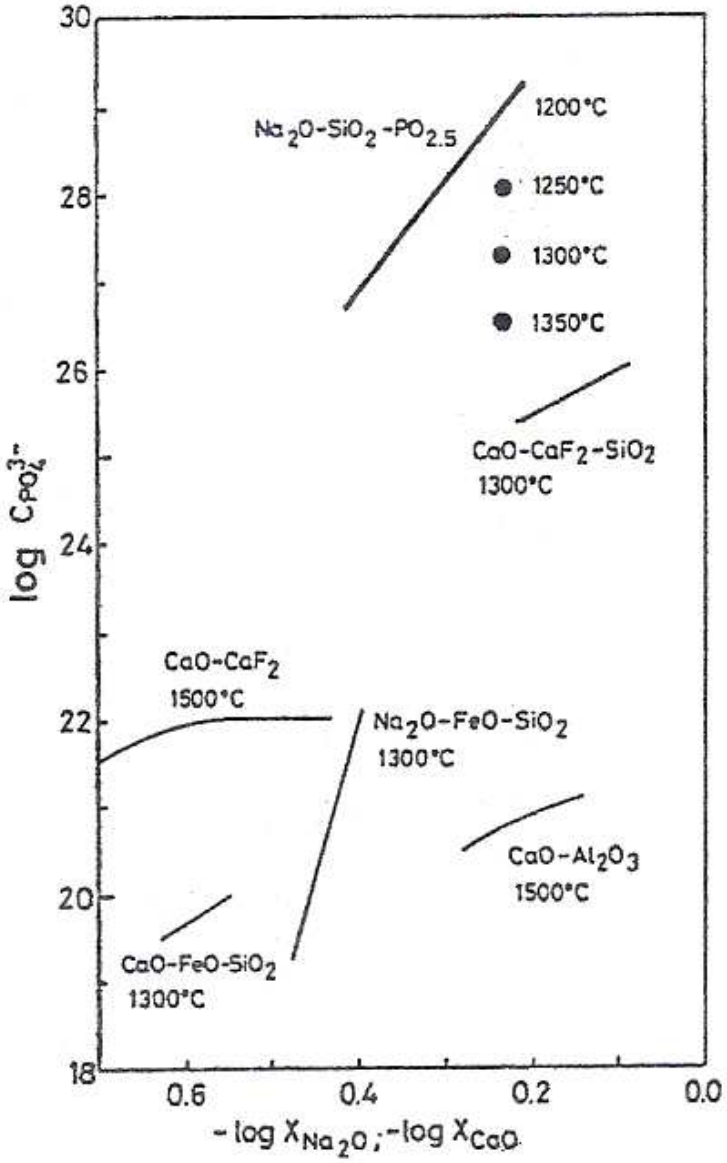



**Figure 2.4** A comparison of phosphate capacities of various systems[11]

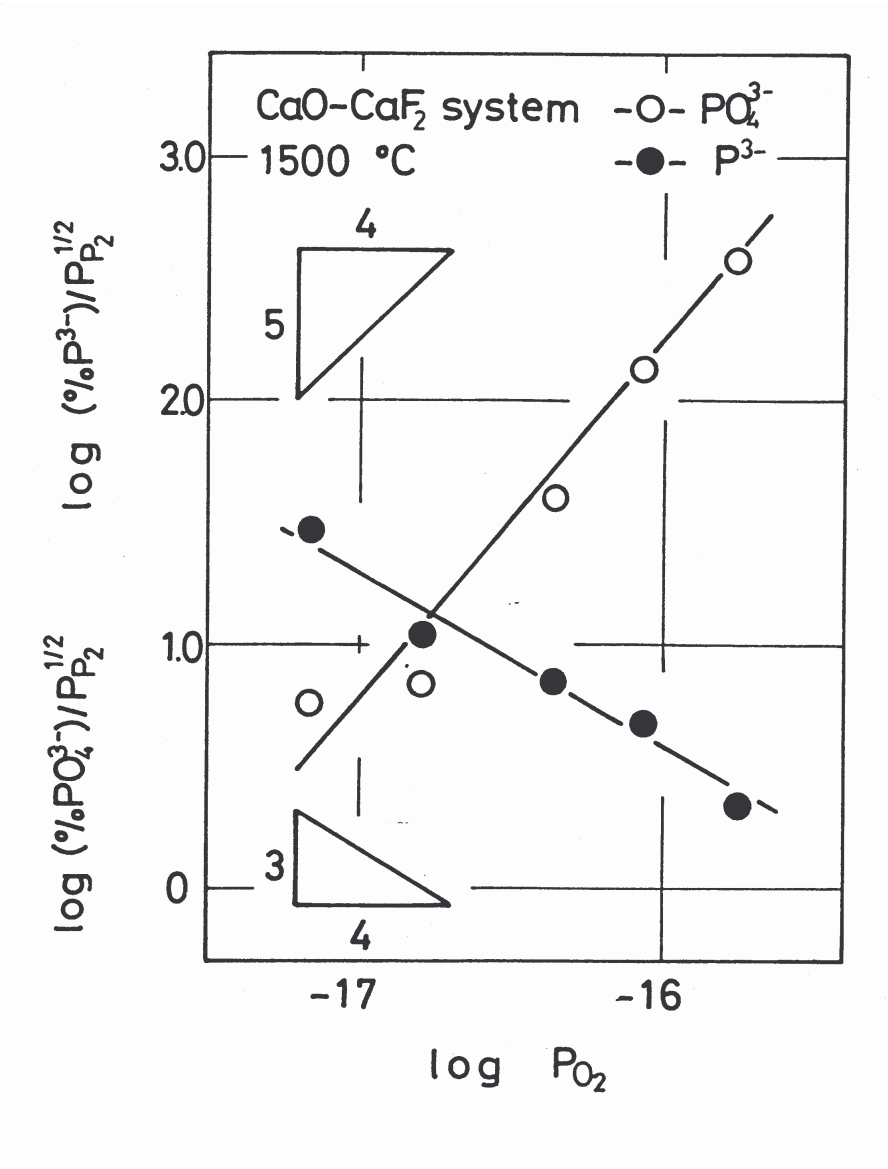



**Figure 2.5** $(\%PO_4^{3-})/(P_{P_2}^{1/2})$ and $(\%P^{3-})/(P_{P_2}^{1/2})$ in the $CaO_{(sat)}$-$CaF_2$ melt as a function of Log $Po_2$[13]

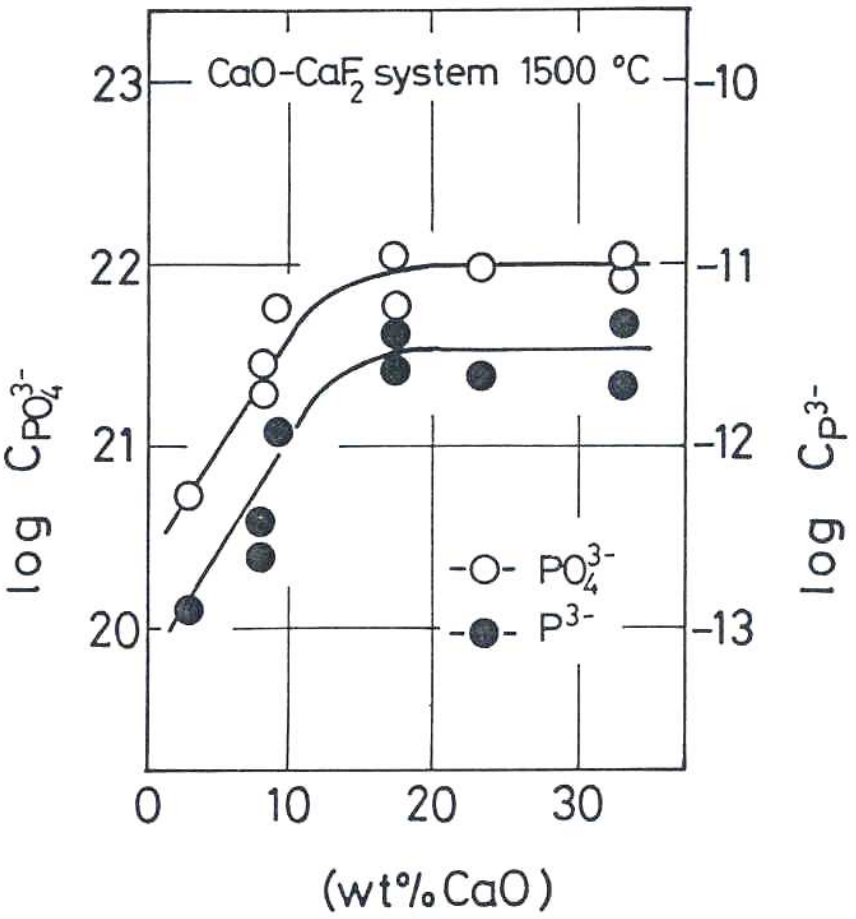



**Figure 2.6** Phosphate and phosphide capacities against wt. % CaO for the $CaO\text{-}CaF_2$ system[13]

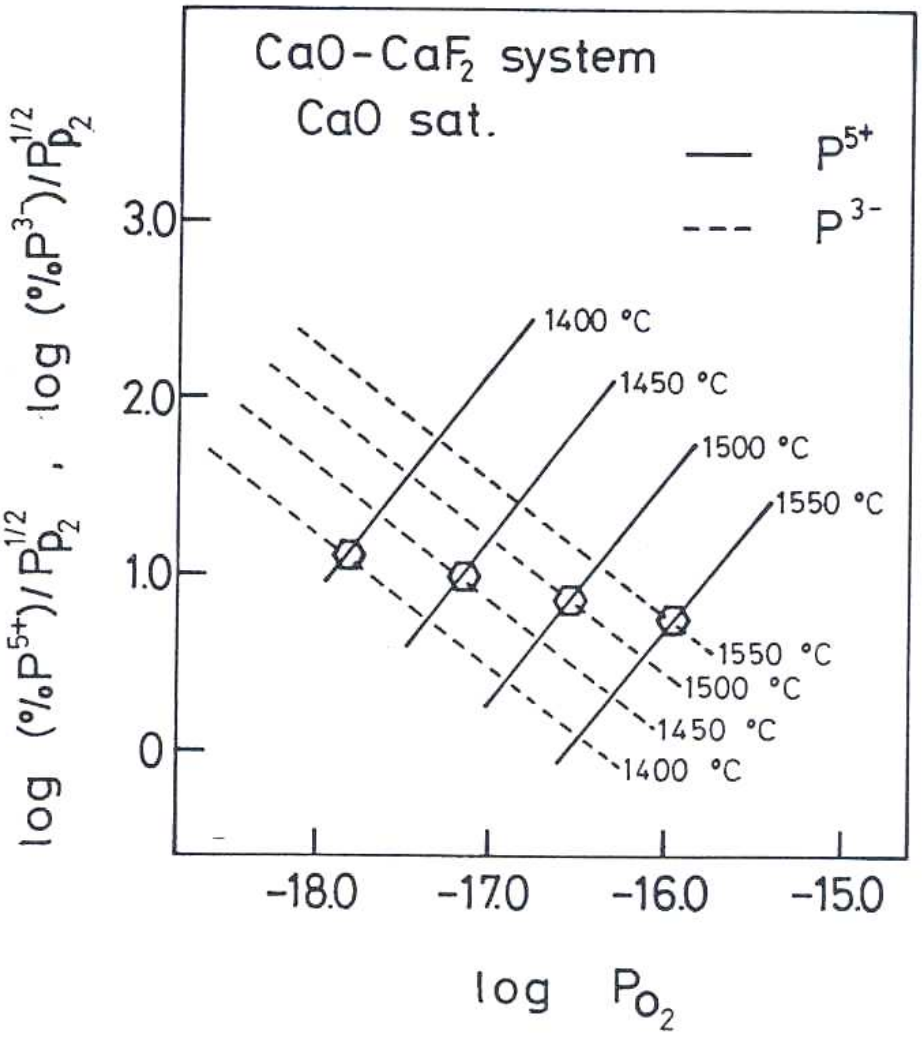



**Figure 2.7** Stability of phosphate and phosphide ions for the CaO-$CaF_2$ system saturated with CaO as a function of log $Po_2$[13]

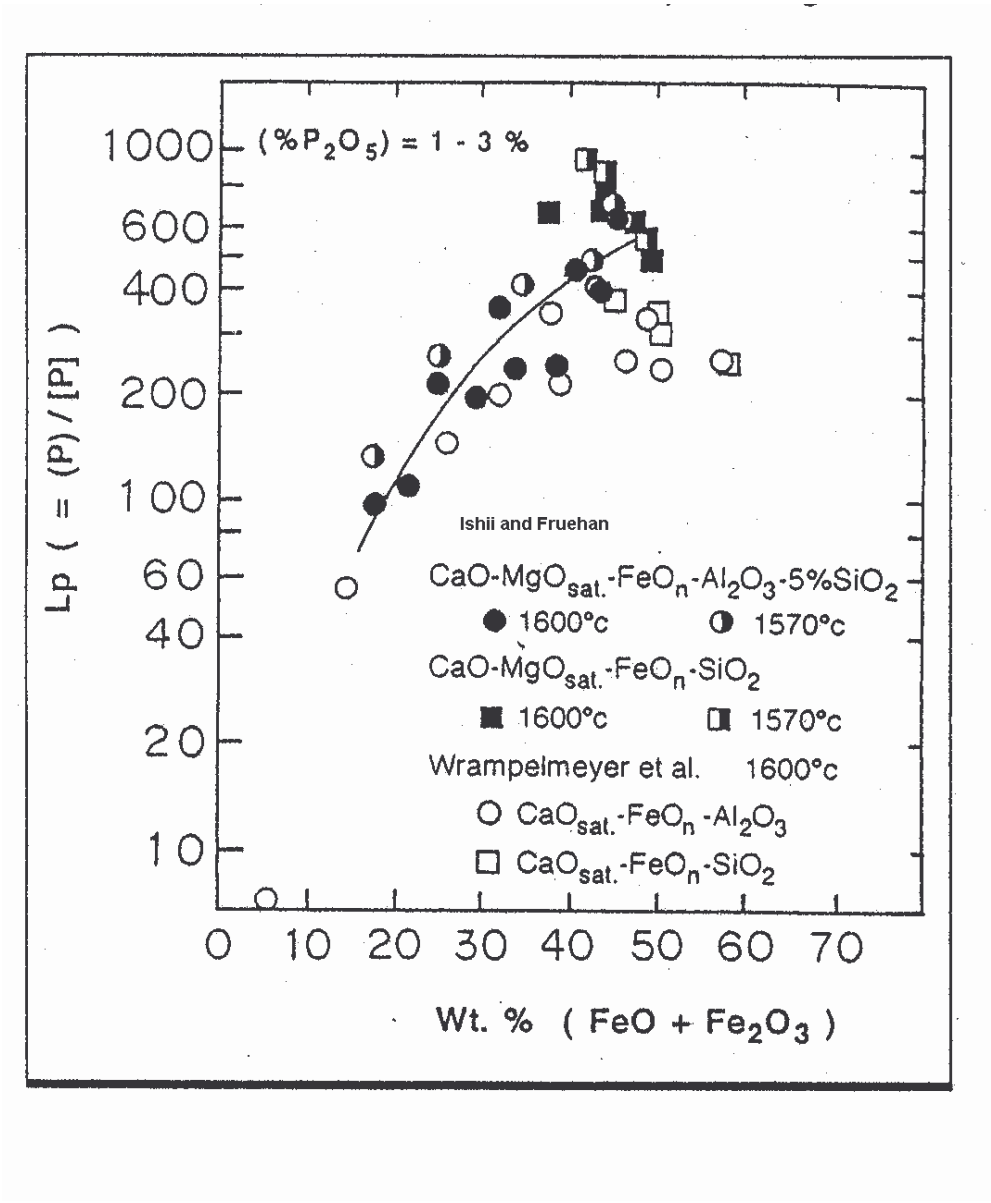



**Figure 2.8** Phosphorus distribution ratios as a function of wt. % $(FeO_n)$[25]

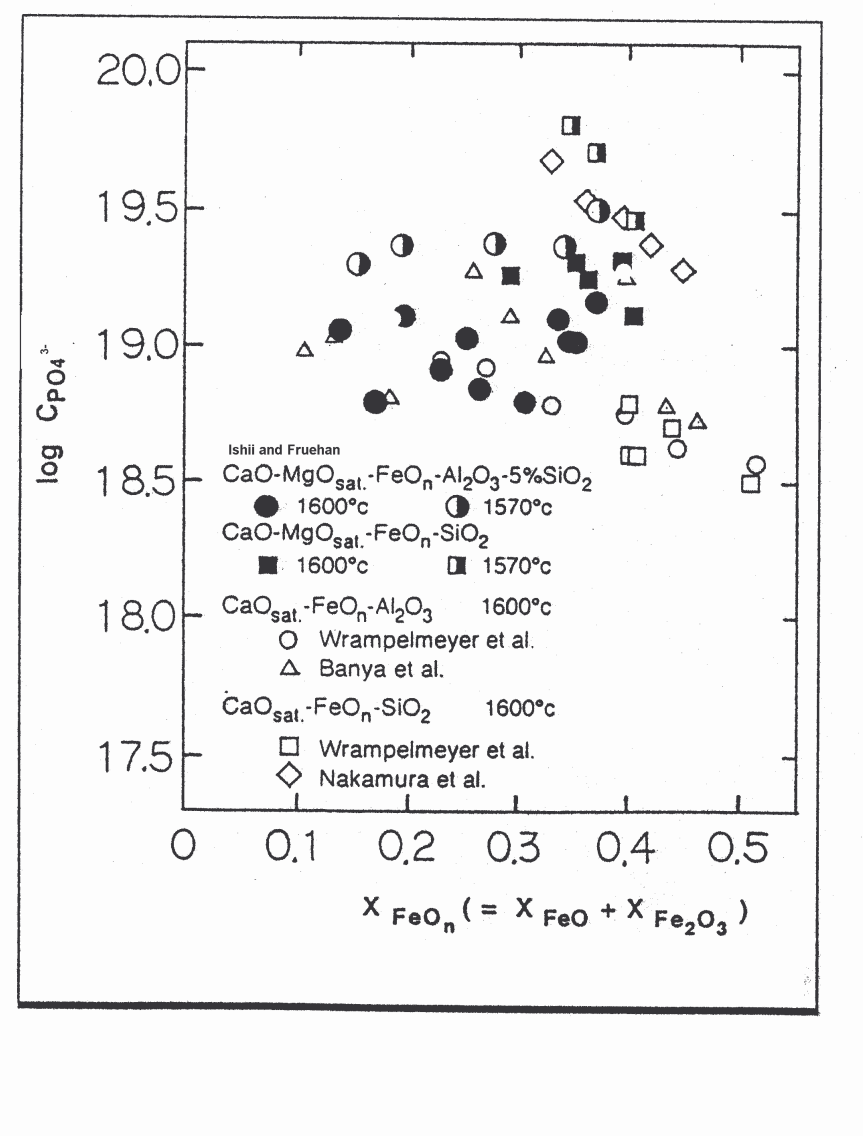



**Figure 2.9** The relationship between $(\log C_{PO_4^{3-}})$ and mole fraction of $FeO_n(X_{FeOn})$[25]

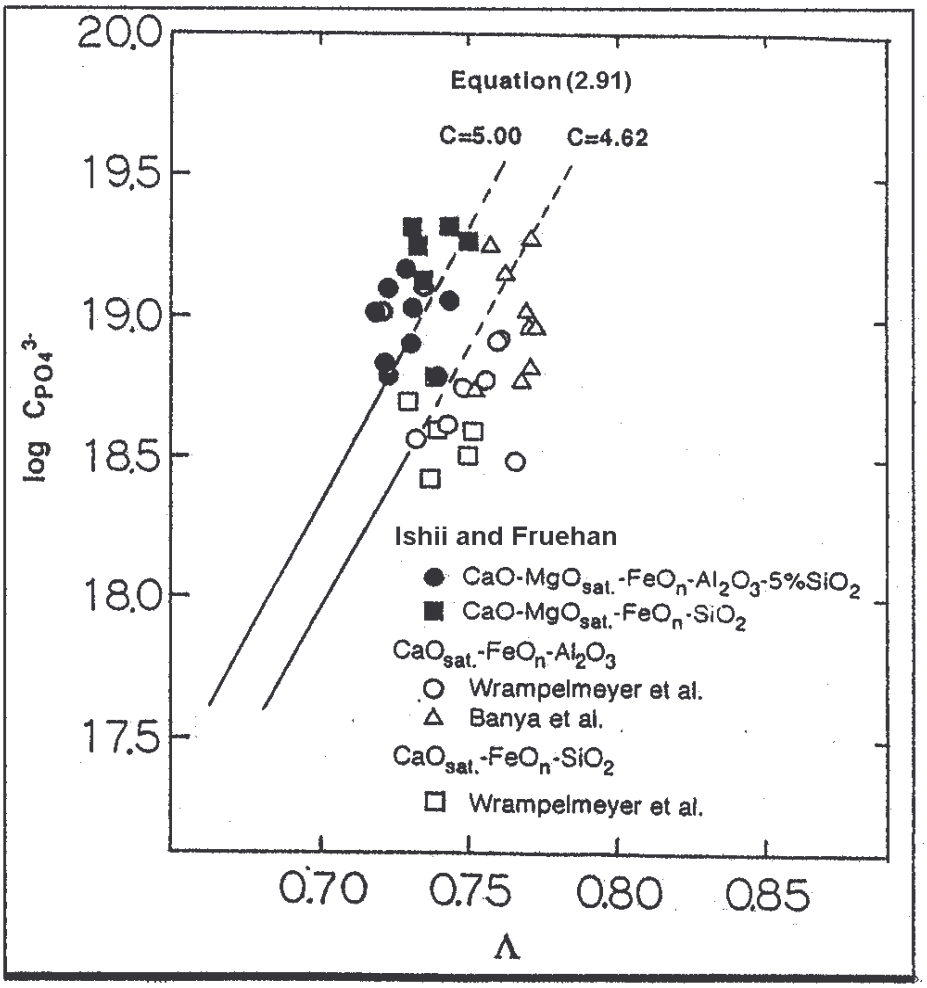



**Figure 2.10** Relation between the optical basicity, Λ and $\log C_{PO_4^{3-}}$ for highly basic slags at 1600°C [25]

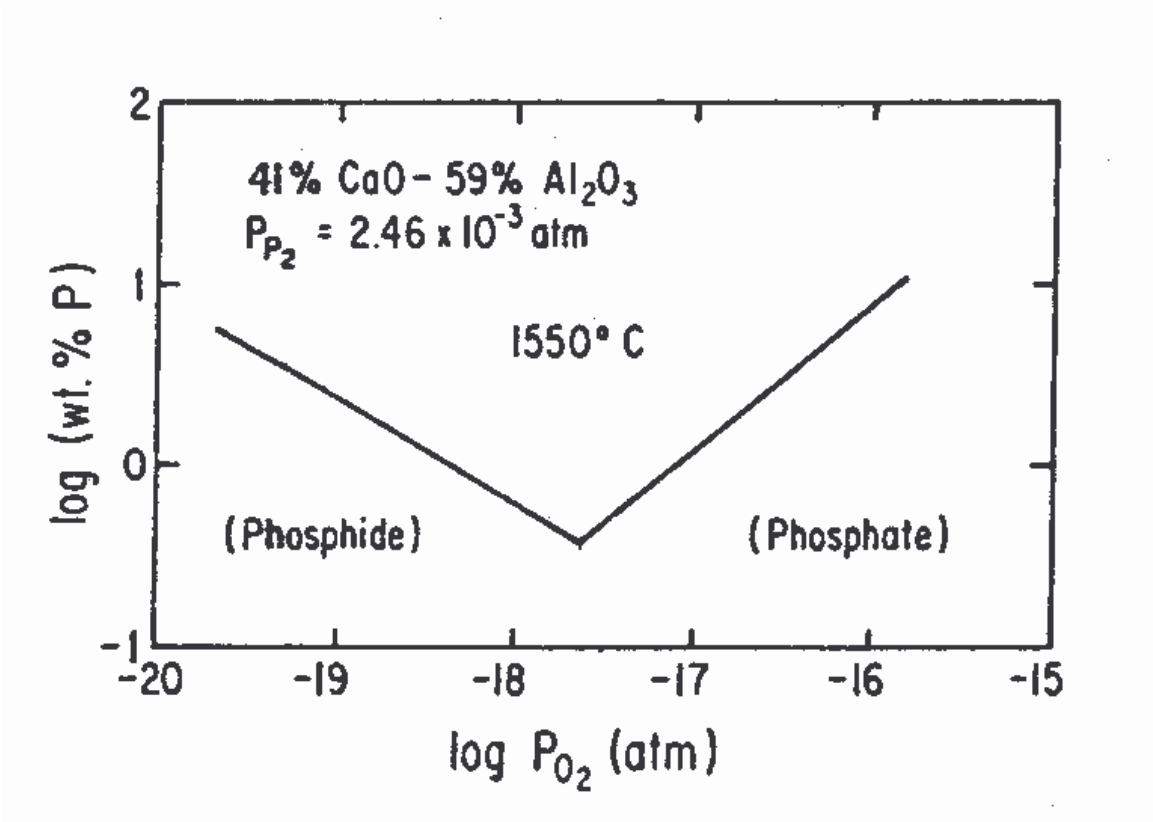



**Figure 2.11** Phosphide/ phosphate solubilities in a calcium aluminate slag[12]

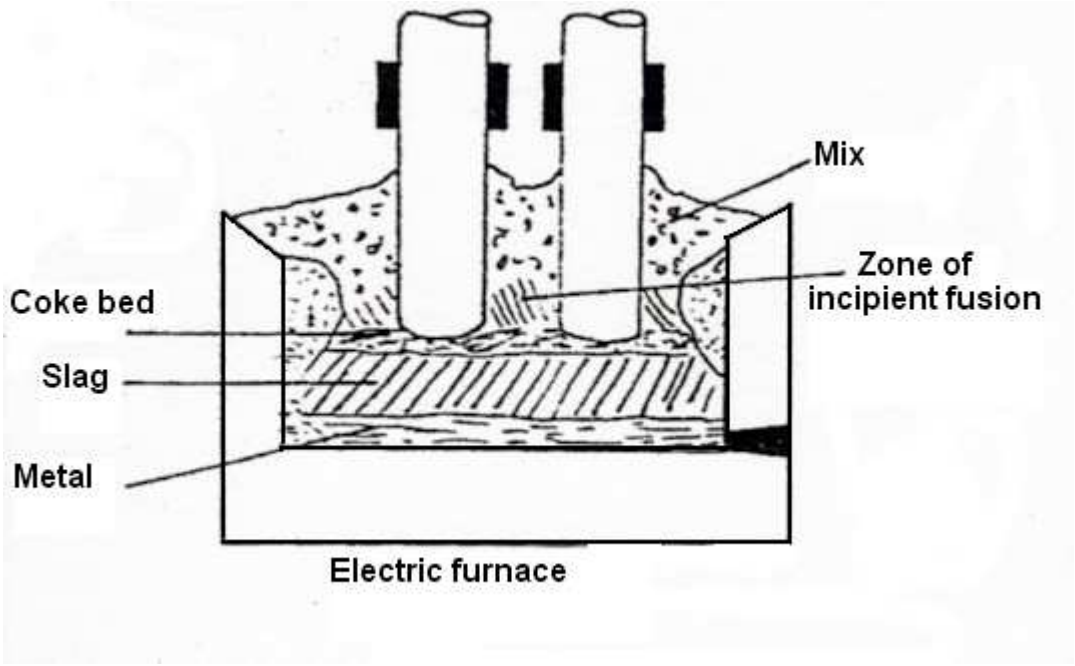



**Figure 2.12** Schematic diagram of the electric furnace showing zone of incipient fusion[44]

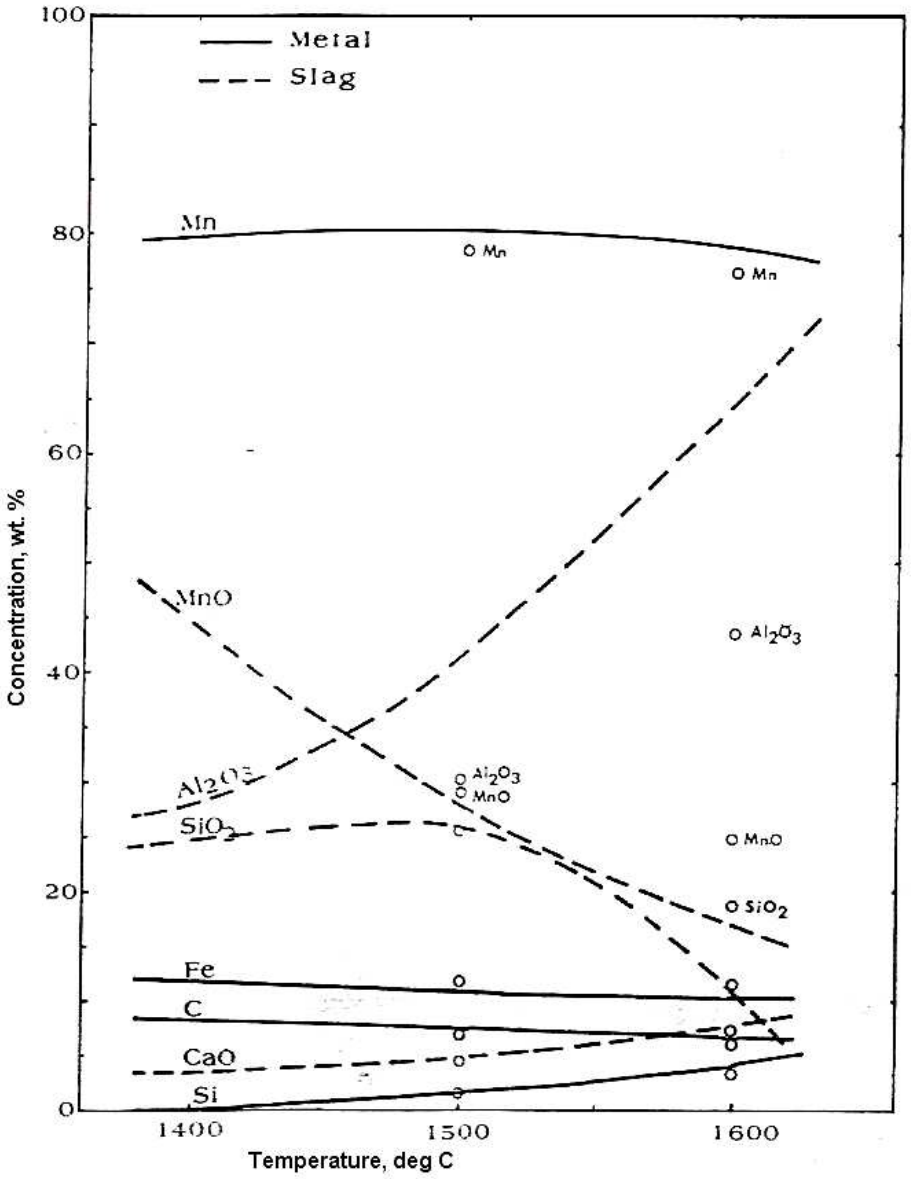



**Figure 2.13** Variation of metal and slag composition with temperature at carbon saturation condition[47]

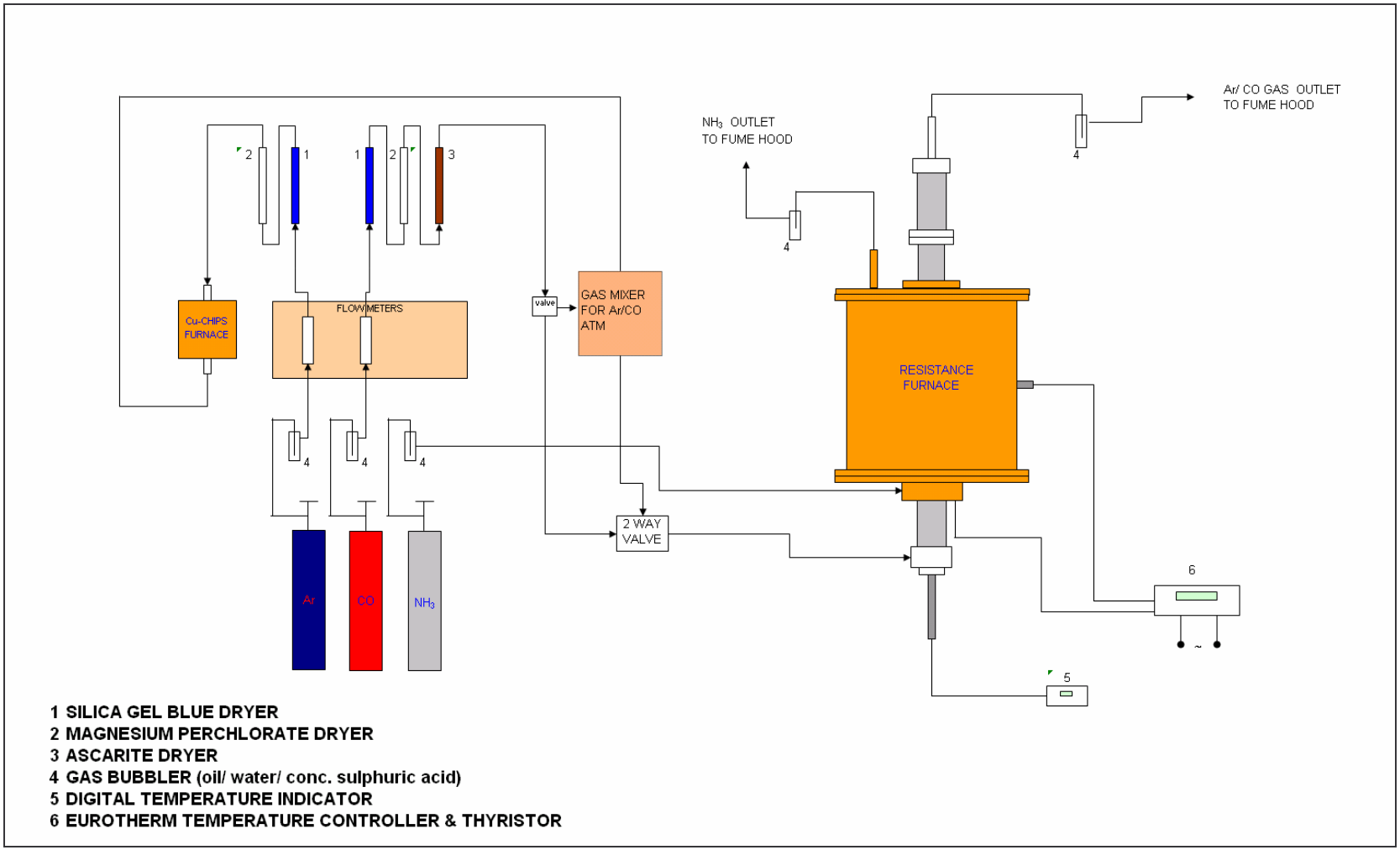



**Figure 3.1:** Flow diagram of the experimental set-up

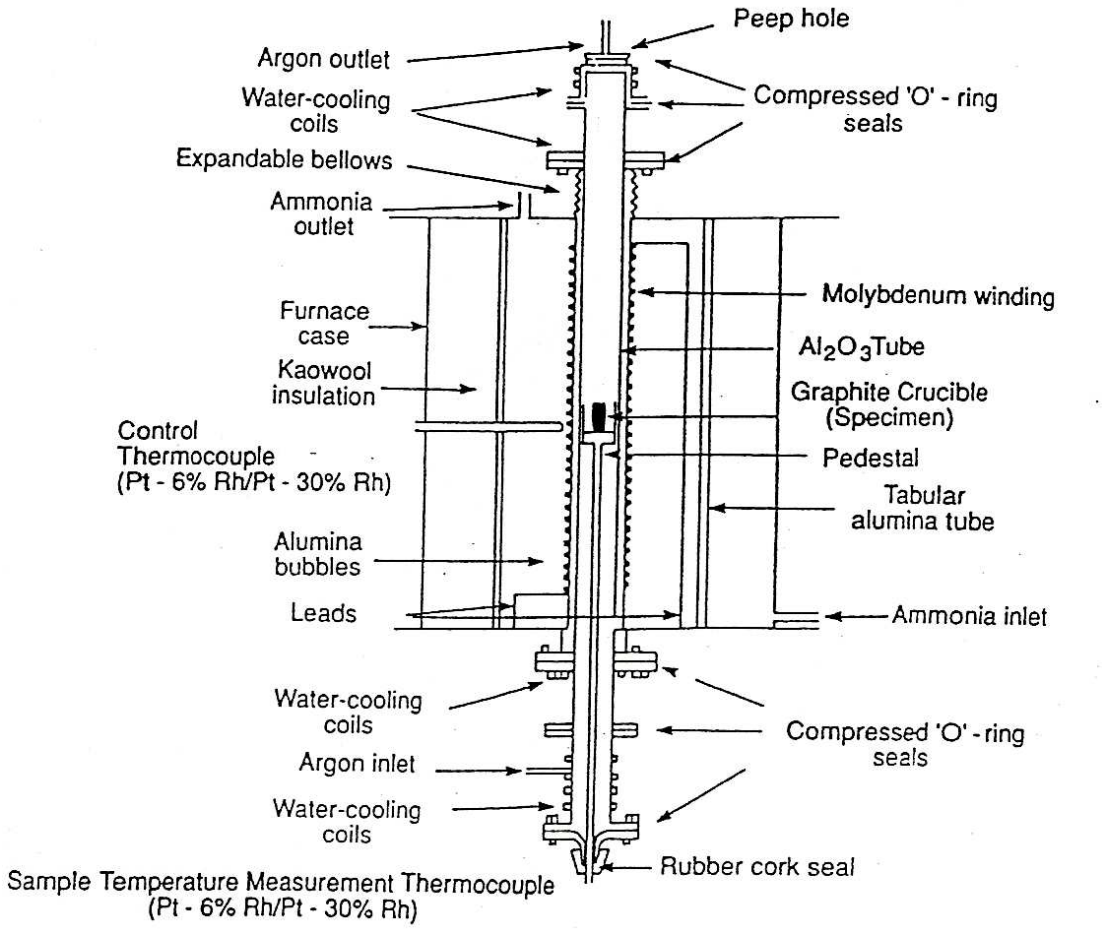



**Figure 3.2:** A cross section of the vertical molybdenum wound resistance furnace.